

Supporting Information

Identification and Interrogation of the Herbicidin Biosynthetic Gene Cluster: First Insight into the Biosynthesis of a Rare Undecose Nucleoside Antibiotic

Geng-Min Lin, Anthony J. Romo, Priscilla H. Liem, Zhang Chen, Hung-wen Liu*

S1.	Experimental Methods	2
S1.1.	General	2
S1.2.	Production and Isolation of Herbicidins	3
S1.3.	Feeding Studies	3
S1.4.	Genome Sequencing and Analysis	3
S1.5.	Cosmid Library Construction and Screening	4
S1.6.	Heterologous Expression	4
S1.7.	Hydrolysis of Herbicidin A	5
S1.8.	Overexpression and Purification of <i>N</i> -His ₆ -tagged Her8	6
S1.9.	Overexpression and Purification of Her10	6
S1.10.	Activity Assay of Methyltransferases	6
S2.	Production and Isolation of Herbicidins	8
S3.	Feeding Studies	10
S3.1.	Peripheral Modifications	10
S3.2.	Core Assembly	10
S4.	Identification of the Gene Cluster	14
S5.	Heterologous Expression	16
S6.	Proposed Functions of Enzymes Encoded in the Cluster	18
S7.	Activity Assay of Methyltransferases	21
S7.1.	Hydrolysis of Herbicidin A	21
S7.2.	Purification of Two Methyltransferases	21
S7.3.	Activity Assay of Methyltransferases	22
S8.	References	25
	Appendix (NMR Spectra)	23

S1. Experimental Methods

S1.1. General

Reagents. All chemical reagents were purchased from commercial sources and used without further purification unless otherwise specified. ^{13}C -labeled materials were purchased from Cambridge Isotope Laboratories (Tewksbury, MA), oligonucleotides from Integrated DNA Technologies (Coralville, IA), KOD Hot Start DNA Polymerase Kit from EMD Millipore (Billerica, MA), QIAprep[®] Miniprep Kit from Qiagen (Valencia, CA), Monarch[®] DNA Gel Extraction Kit from New England Biolabs (Ipswich, MA), PureLink[®] Genomic DNA Mini Kit from Invitrogen (Carlsbad, CA), and Gigapack III XL Packaging Extract from Agilent Technologies (Santa Clara, CA). The concentration of each of the herbicidins was determined by measuring its absorption at 260 nm and calibrated based on the extinction coefficient of adenine at 260 nm ($\epsilon_{260} = 17,000 \text{ cm}^{-1}\text{M}^{-1}$).

Instruments. NMR spectra were recorded using a Varian Direct Drive 600 MHz NMR, a Varian Inova 500 MHz NMR, a Bruker Avance III HD 500 MHz NMR equipped with CryoProbe[™] Prodigy, or an Agilent MR 400 MHz NMR spectrometer at the Nuclear Magnetic Resonance Facility of The University of Texas at Austin. ^{13}C NMR spectra were recorded under proton broad-band decoupling. Deuterated solvents were used as the internal reference for all acquired NMR spectra. NMR spectra were processed and plotted using MestReNova 10 (Mestrelab Research S.L.). Electrospray ionization mass spectra (ESI-MS) were acquired using an Agilent 6230 Accurate-Mass ToF LC/MS with an Agilent 1260 liquid chromatography (LC) module. High-performance liquid chromatography (HPLC) was performed using a Beckman System Gold 125 Solvent Module with a 166 detector equipped with a C18 reversed-phase column (Microsorb 100-5 C18 S250×4.6, Agilent Technologies). Silica gel column chromatography was carried out using SiliaFlash P60 (230 – 400 mesh, Silicycle).

Bacterial Strains and Plasmids. *Streptomyces* sp. L-9-10 was a generous gift from Prof. Julian Davies at The University of British Columbia. *Streptomyces albus* J1074 was generously provided by Prof. Ben Shen at The Scripps Research Institute. *Streptomyces* strains were preserved as a mycelial suspension or spore suspension in 20% glycerol at $-80\text{ }^{\circ}\text{C}$.¹ *Escherichia coli* DH5a was used for routine cloning experiments, and BL21 star (DE3) as the protein overexpression host. The *E. coli* XL-1 MRF' strain was used for construction of the cosmid library, and *E. coli* S17-1 was used for intergeneric conjugal transfer of cosmid DNA.² Plasmid pOJ446³ was used for construction of the cosmid library, and pET28b(+) and malE-pET were used for protein overexpression in *E. coli*. Apramycin, kanamycin, nalidixic acid, streptomycin, and tetracycline were used at concentrations of 15–50 $\mu\text{g}/\text{mL}$, 30–50 $\mu\text{g}/\text{mL}$, 50 $\mu\text{g}/\text{mL}$ (in 0.3 N NaOH), 10 $\mu\text{g}/\text{mL}$, and 15 $\mu\text{g}/\text{mL}$ (in 70% EtOH), respectively.

HPLC Conditions. High-performance liquid chromatography (HPLC) analysis and purification were performed using a C18 reversed-phase column (Microsorb 100-5 C18 S250×4.6, Agilent Technologies), and the samples were eluted with a two-solvent system of A, 0.1% formic acid in water, and B, 0.1% formic acid in acetonitrile. The flow rate was 1 mL/min and elution was monitored using a UV-detector set at 260 nm, which is the maximum absorption wavelength for adenine. Sample elution started with a linear gradient from 15–30% B over 20 min, followed by another gradient from 30–80% B over 2 min. After staying at 80% B for another 5 min, the eluent was brought back to 15% B within 3 min and equilibrated at 15% B for another 10 min before the next injection.

S1.2. Production and Isolation of Herbicidins

Approximately 100 μL of a mycelial suspension of *Streptomyces* sp. L-9-10 was used to inoculate 10 mL of autoclaved media composed of 0.5% yeast extract, 0.5% malt extract, 1.5% soytone, 1% glucose, 0.3% sodium chloride, 1.5% glycerol, 0.1% Tween[®] 80, 0.3% antifoam SE-15 (Sigma-Aldrich), and 2% 3-morpholinopropane-1-sulfonic acid (MOPS) buffer at pH 7. This seeding culture was allowed to grow at 28 – 30 °C shaken at 200 rpm for two days, and 1 mL of the resulting culture was used to inoculate 100 mL of autoclaved media with the identical composition to the seeding culture. This culture was then grown under the same conditions as the seeding culture for another 5 days prior to the isolation of herbicidin A and 7 days for herbicidin B.

After pelleting the cellular material via centrifugation (4000 $g \times 15$ min), the supernatant was washed with hexanes (100 mL), followed by extraction with EtOAc (100 mL $\times 2$) and *n*-butanol (100 mL). The combined organic layers were evaporated under reduced pressure and then chromatographed with 20 mL (dry volume) of Diaion HP-20 (40 – 90% aqueous MeOH). Herbicidins were usually eluted at 50 – 70% MeOH. Fractions containing the desired compounds were pooled, dried, and purified further with silica gel (10 g, 5 – 12.5% MeOH in CH_2Cl_2) to yield herbicidins A and B as white to pale yellow solids. The yields of herbicidins A and B were typically around 5–10 mg from a 100 mL culture. R_f values for herbicidins A and B based on thin layer chromatography (TLC) were approximately 0.33 and 0.17, respectively, when developed using 10% MeOH in CH_2Cl_2 .

S1.3. Feeding Studies

The cultures were prepared as described in Section S1.2. ¹³C-labeled materials, including [^{U-¹³C}]glucose, [1-¹³C]glucose, [6-¹³C]glucose, [^{U-¹³C}]ribose, [5-¹³C]ribose, [^{U-¹³C}, ¹⁵N]isoleucine, [Me-¹³C]methionine, and sodium [2-¹³C]acetate, were prepared separately as 200 mM stock solutions and filter-sterilized. Stock solution (500 μL) of a given labeled compound was added to the culture on the second, third, and fourth days of incubation. The final concentration of labeled material was 3 mM. Herbicidin A was then isolated from the culture supernatant as described above, and the ¹³C enrichment was analyzed by ¹³C NMR.

S1.4. Genome Sequencing and Analysis

Genomic DNA of *Streptomyces* sp. L-9-10 was isolated according to the instructions provided by the PureLink[®] Genomic DNA Mini Kit from Invitrogen (Carlsbad, CA). It was then submitted to The Genome Sequencing and Analysis Facility of The Institute of Cellular and Molecular Biology at The University of Texas at Austin. The sequencing was done on an Illumina MiSeq[®] sequencer using a 2 \times 300 bp paired-end library targeting a minimum of 2 million reads.

The raw data was trimmed using *BBDuk* tools in the *BBMap* software package developed by Brian Bushnell.⁴ Any sequence beyond the common adapter of Illumina (GATCGGAAGA) at the 3'-end was trimmed for each read, and the paired read was also trimmed accordingly. Reads from the common PhiX spike-in for sequencing control on the Illumina platform were then removed. The trimmed data were assembled using the *Velvet* assembler,⁵ and the parameters for assembly were optimized using *Velvetoptimiser*.⁶

The assembled raw data were submitted to the Rapid Annotation using Subsystem Technology (RAST) webserver for annotation.⁷ The annotated draft genome was then download as a GenBank file, and the putative gene clusters therein were predicted using antiSMASH.⁸ Protein-encoding genes in the putative gene cluster were further analyzed using Basic Local Alignment Search Tool (BLAST) from the National Center for Biotechnology Information (NCBI).

The draft genome contains 178 contigs with N50 of 203,880, covering ca. 8.8 million base pairs. Among the 7,735 genes encoded in the draft genome, about 30 putative biosynthetic clusters were identified by antiSMASH 3.0.

S1.5. Cosmid Library Construction and Screening

Genomic DNA of *Streptomyces* sp. L-9-10 was partially digested with *Sau3AI*. Digested DNA fragments were purified via phenol-chloroform-isoamyl alcohol (PCI) extraction, followed by KOAc-¹PrOH precipitation, and ligated with pOJ446 pre-digested with *HpaI* and *BamHI*. The ligation reaction products were purified with PCI extraction and KOAc-¹PrOH precipitation, and packaged into phage particles using a Gigapack III XL Packaging Extract from Agilent Technologies (Santa Clara, CA) according to manufacturer's instructions. The packaged phage solution was kept at 4 °C before use. The recipient *E. coli* XL-1 MRF' was grown in LB media supplemented with 0.2% maltose and 10 mM MgSO₄ until the optical density at 600 nm (OD₆₀₀) reached 0.5. The cell pellet was harvested via centrifugation and suspended in 10 mM MgSO₄. The pre-made packaging solution was diluted 1 : 1 or 1 : 10 with SM buffer (0.1 M NaCl, 0.2% MgSO₄, 0.01% gelatin, 50 mM Tris-HCl, pH 7.5) before being mixed with an equal volume of *E. coli* suspension. Transduction was carried out at room temperature for 30 min, and LB (1 mL) was then added for recovery. The culture was incubated at 37 °C for another 1 h before being plated onto LB agar plates supplemented with apramycin (50 µg/mL) and incubated overnight at 37 °C to select for transductants. The genomic library consisted of around 5,000 cosmids generated from two transduction experiments.

Two sets of polymerase chain reaction (PCR) primers were designed as probes to screen the cosmid library as shown in Table S1. One set of primers (GML01/GML02) was designed to amplify a 522 bp region upstream from the putative gene cluster. The second set (GML03/GML04) was designed to amplify a 630 bp region downstream from the cluster. Among 1,300 cosmids screened, only one cosmid, L8B17, was positive against both sets of primers. The cosmid was purified and sequenced using primers GML05/06 to identify the boundary of the inserted genomic fragment, which was then mapped onto the draft genome.

Table S1. Annotation and predicted function of genes in the her cluster. *The length of predicted peptides. XDH: xanthine dehydrogenase. G3PDH: glyceraldehyde 3-phosphate dehydrogenase.

number	name	sequence
GML01	her-up-f	5'-TGCGTGCCGATGACCGACAGC-3'
GML02	her-up-r	5'-GCAGAGCATCCTCGACCTGCTGC-3'
GML03	her-down-f	5'-GAGGATGGTCGCCTGCACCCGGTC-3'
GML04	her-down-r	5'-ATGACCCTCACCGTGGTGGTCGTCGA-3'
GML05	pOJ446-f	5'-GTCATAAGTGCGGCGACGATAGTC-3'
GML06	pOJ446-r	5'-TACCACGGCCTCTGACGGCT-3'

S1.6. Heterologous Expression

Intergeneric transfer of cosmid L8B17 and empty vector pOJ446 from *E. coli* S17-1⁹ to *S. albus* J1074 was carried out following a standard protocol with minor modification.¹ The cosmid L8B17 was first transformed into *E. coli* S17-1. A single colony was used to inoculate LB media (50 µg/mL apramycin and 10 µg/mL streptomycin). After growing overnight at 37 °C, the culture was diluted 50 times into an identical media and grown at 37 °C until the OD₆₀₀ reached 0.5. The cellular material was pelleted via centrifugation and resuspended in an equal volume of LB media. The washing process was repeated twice to remove antibiotics, and the *E. coli* cell pellet was eventually resuspended in 1/10 the original culture volume of LB media before conjugation. At

the same time, the spore stock of *S. albus* J1074 was heat-shocked at 50 – 55 °C for 10 min. Spores (ca. 2×10^8 , estimated by OD₄₅₀, where OD = 1 correspond roughly to 3.3×10^8 spores/mL) were then mixed with 2×10^7 , 2×10^8 , or 2×10^9 resuspended *E. coli* cells (estimated by OD₆₀₀, where OD = 1 corresponds to approximately 8×10^8 cells/mL). The mixture was vortexed and plated onto ISP4 plates supplemented with 30 mM MgCl₂. The conjugation plates were incubated at 30 °C for 16 h, which were then overlaid with 2.5 mL of soft agar¹⁰ supplemented with antibiotics to make the final concentration of apramycin and nalidixic acid both equal to 50 µg/mL.

After 3 – 5 days, colonies started to appear, and several single colonies were streaked onto new R2YE plates with 50 µg/mL each of apramycin and nalidixic acid. Colonies grown on the second plate were further confirmed by successful PCR amplification of predicted fragments from the extracted cosmid DNA using the primers listed in Table S1, and the *Bam*HI restriction pattern. The desired exoconjugants were then subjected to the production conditions described in Section S1.2 except that 15 µg/mL of apramycin and 50 µg/mL of nalidixic acid were supplemented in all of the media. The cultures were monitored for up to 14 days and aliquots were taken out and worked up for HPLC analysis every 2 days.

S1.7. Hydrolysis of Herbicidin A

A solution containing 1 mM herbicidin A (**1a**) and 100 mM LiOH in 1 mL of tetrahydrofuran/water (*v/v* = 3/1) was incubated at room temperature for 2.5 h. The reaction was then neutralized with diluted acetic acid and concentrated to remove volatile organic solvent. The mixture was then purified using HPLC to yield **9** and **10** both as white solids.

Spectroscopic characterization of **9**: ¹H NMR (CD₃OD, 400 MHz) δ 1.99 (d, *J* = 7.0 Hz, 3H, H-4''), 2.20 (br t, *J* = 12.0 Hz, 1H, H-5'), 2.34 (br dd, *J* = 12.0, 5.6 Hz, 1H, H-5'), 3.41 (s, 3H, OMe), 4.00 (br s, 1H, H-2'), 4.27 (br s, 1H, H-10'), 4.33 – 4.51 (m, 5H, H-3', H-4', H-9', and H-5''), 4.65 (dd, *J* = 12.0, 5.6 Hz, 1H, H-6'), 5.08 (d, *J* = 2.8 Hz, 1H, H-8'), 6.04 (s, 1H, H-1'), 6.97 (q, *J* = 7.1 Hz, 1H, H-3''), 8.01 (s, 1H, H-2), 8.19 (s, 1H, H-8). ¹H NMR (D₂O, 500 MHz) 1.82 (d, *J* = 7.0 Hz, 3H, H-4''), 2.17 (br t, *J* = 12.0 Hz, 1H, H-5'), 2.32 (br d, *J* = 12.0 Hz, 1H, H-5'), 3.40 (s, 3H, OMe), 4.21 (br s, 3H, H-2' and H-5''), 4.32 (br s, 1H, H-10'), 4.39 (dd, *J* = 3.0, 1.0 Hz, 1H, H-9'), 4.43 (dd, *J* = 12.0, 5.5 Hz, 1H, H-6'), 4.52 (br s, 2H, H-3' and H-4'), 4.93 (d, *J* = 3.0 Hz, 1H, H-8'), 5.97 (d, *J* = 1.5 Hz, 1H, H-1'), 6.77 (q, *J* = 7.0 Hz, 1H, H-3''), 8.00 (s, 1H, H-2), 8.23 (s, 1H, H-8). HRMS (ESI) *m/z* calcd for C₂₂H₂₇N₅O₁₁ ([M + H]⁺) 538.1780; found 538.1790.

Spectroscopic characterization of the hemiacetal form of **10**: ¹H NMR (CD₃OD, 400 MHz) δ 2.19 (td, *J* = 11.6, 3.4 Hz, 1H, H-5'), 2.27 (br d, *J* = 11.6 Hz, 1H, H-5'), 3.45 (s, 3H, OMe), 3.70 (d, *J* = 3.2 Hz, 1H, H-8'), 3.98 (br s, 1H, H-2'), 4.26 (br s, 1H, H-10'), 4.38 – 4.42 (m, 2H, H-4' and H-9'), 4.43 (br d, *J* = 2.4 Hz, 1H, H-3'), 4.63 (dd, *J* = 11.6, 5.2 Hz, 1H, H-6'), 6.15 (s, 1H, H-1'), 8.19 (s, 1H, H-2), 8.73 (s, 1H, H-8). ¹H NMR (D₂O, 500 MHz) δ 2.19 (ddd, *J* = 14.0, 13.0, 3.5 Hz, 1H, H-5'), 2.28 (ddd, *J* = 14.0, 4.0, 2.5 Hz, 1H, H-5'), 3.42 (s, 3H, OMe), 3.69 (d, *J* = 3.0 Hz, 1H, H-8'), 4.16 (br s, 1H, H-2'), 4.21 (br s, 1H, H-10'), 4.41 (dd, *J* = 3.0, 1.3 Hz, 1H, H-9'), 4.46 – 4.55 (m, 3H, H-3', H-4', and H-6', overlapped with H-4' from acyclic form), 6.13 (d, *J* = 1.0 Hz, 1H, H-1'), 8.26 (s, 1H, H-2), 8.56 (s, 1H, H-8).

Spectroscopic characterization of the free carbonyl form of **10**: ¹H NMR (D₂O, 500 MHz) δ 2.17 – 2.25 (m, 1H, H-5'), 2.40 – 2.50 (m, 1H, H-5'), 3.44 (s, 3H, OMe), 3.73 (dd, *J* = 10.0, 9.0 Hz, 1H, H-9'), 3.93 (d, *J* = 10.0 Hz, 1H, H-8'), 4.02 (dd, *J* = 12.6, 6.0 Hz, 1H, H-6'), 4.09 (d, *J* = 9.0 Hz, 1H, H-10'), 4.29 (s, 1H, H-2'), 4.44 (d, *J* = 2.0 Hz, 1H, H-3'), 4.46 – 4.55 (m, 1H, H-4', overlapped with H-3', H-4', and H-6' from free carbonyl form), 6.12 (d, *J* = 1.5 Hz, 1H, H-1'),

8.27 (s, 1H, H-2), 8.40 (s, 1H, H-8). HRMS (ESI) m/z calcd for $C_{17}H_{21}N_5O_9$ ($[M + H]^+$) 440.1412; found 440.1412.

S1.8. Overexpression and Purification of *N*-His₆-tagged Her8

The gene encoding Her8 with additional nucleotides upstream and downstream was first amplified from genomic DNA of *Streptomyces* sp. L-9-10 using primers GML07/08. The purified PCR product then served as the template for PCR-amplification of the *her8* gene using primer pairs GML09/10. The target genes with engineered restriction sites were then ligated with pCR[®]-Blunt vector pre-digested with *Stu*I, and then sub-cloned into the *Nde*I/*Hind*III sites of pET28b(+) to generate the *her8*/pET28b(+) plasmid. These constructs were confirmed by sequencing using T7 and T7-terminal primers.

Plasmid *her8*/pET28b(+) was then transformed into *E. coli* BL21 star (DE3). A single colony containing the desired plasmid was used to inoculate 10 mL of LB broth containing 50 µg/mL kanamycin, which was grown overnight at 37 °C at 200 rpm. This overnight culture was then used to inoculate 1 L of LB media containing 30 µg/mL kanamycin. The culture was allowed to grow at 37 °C at 200 rpm until the OD₆₀₀ reached 0.5 – 0.6, at which time isopropyl-D-1-thiogalactopyranoside (IPTG) was added to a final concentration of 0.1 mM to induce protein overexpression. At the same time, the temperature and rotary speed were decreased to 18 °C and 180 rpm, respectively, and the culture was grown under these conditions for another 20 h. Cell pellets were then collected by centrifugation (4000 g × 25 min) and kept at –80 °C before purification.

Thawed cell pellets were resuspended in storage buffer (50 mM Tris-HCl, 15% glycerol, pH 8) supplemented with 10 mM imidazole and sonicated to disrupt the cells. The supernatant was collected following centrifugation and equilibrated with ca. 1 mL pre-washed Ni-NTA beads for at least one hour at 4 °C. After washing out unbound proteins from the beads, non-specifically bound proteins were eluted using storage buffer containing 20 mM imidazole. *N*-His₆-tagged Her8 was then eluted using storage buffer with 250 mM imidazole. Pooled proteins were dialyzed against storage buffer several times, snap-frozen, and stored at –80 °C. Protein concentrations were determined by Bradford assay using bovine serum albumin (BSA) as the standard,¹¹ and protein purity was assessed by SDS-PAGE.

S1.9. Overexpression and Purification of Her10

The gene encoding Her10 was amplified from *Streptomyces* sp. L-9-10 directly using the primer pair GML11/12 and cloned into *Nde*I/*Hind*III site of malE-pET vector (prepared in-house) to generate plasmid *her10*/malE-pET for the expression of maltose-binding protein (MBP)-fused Her10. Proteins encoded in *her10*/malE-pET were overexpressed and purified as described in Section S1.8. After dialysis, MBP-fused Her10 was treated with 20% His₆-tagged TEV protease (by weight) and incubated at 4 °C overnight to cleave off the His₁₀-tagged MBP. The extent of cleavage was estimated by SDS-PAGE, and more TEV protease was added until most of the fusion protein was cleaved. This protein mixture was then slowly passed through pre-washed Ni-NTA beads, and the beads were further washed with one column volume of storage buffer. Combined flow-through was subjected to the same binding process several times to ensure the complete removal of His₁₀-tagged MBP and His₆-tagged TEV. The final flow-through was concentrated to yield native Her10 with two extra amino acids, Gly-His, at its *N*-terminus.

S1.10. Activity Assay of Methyltransferases

A solution containing 0.5 mM SAM, 100 μ M **9** or **10** in 50 μ L potassium phosphate buffer (50 mM, pH 6.5) was incubated with buffer, 1 μ M of *N*-His₆-tagged Her8, or 1 μ M of Her10 at room temperature for 24 h. The protein was filtered off using YM-10 centrifugal filters, and the filtrate was analyzed by HPLC and ESI-MS.

Table S2. Primers used for constructing plasmids containing *her8* and *her10*. Engineered restriction sites are underlined.

number	name	Sequence
GML07	Her8ex-f	5'-TCAGTACCGGCACACGACACG-3'
GML08	Her8ex-r	5'-GAGCCACTCCGGCGAGAACAG-3'
GML09	Her8-f-NdeI	5'- <u>CATATGGT</u> GAGCGACATCGCGCAGGAC-3'
GML10	Her8-N-r-HindIII	5'- <u>AAGCTT</u> TCAGGACCTCTTGGCCAGGGT-3'
GML11	Her10-f-NdeI	5'- <u>CATATGACT</u> CAGCCGCGGAATGACG-3'
GML12	Her10-N-r-HindIII	5'- <u>AAGCTT</u> CTACTTGACGCCGACGACCAT-3'

S2. Production and Isolation of Herbicidins

Production and isolation of herbicidins from *Streptomyces* sp. L-9-10 have been previously reported in the literature.¹⁸ However, the fermentations were carried out at the 100 L scale for seven days and yielded only 2 – 30 mg of herbicidin variants following multiple extraction methods including size-exclusion chromatography, silica-gel chromatography, and HPLC purification. This was neither feasible nor practical in our laboratory. We were therefore devoted to improve the culture conditions so that we could reliably isolate herbicidin A (**1a**) from a smaller-scale cultures in quantities sufficient for ¹³C NMR analysis in the feeding studies.

We first considered the herbicidin production profile over time. *Streptomyces* sp. L-9-10 was grown under the same conditions as used in the original publication for up to 10 days. Throughout the growth period, an aliquot was taken from the culture each day for HPLC analysis to track the production of herbicidins. As shown in Figure S1, herbicidin A (**1a**) and herbicidin B (**1b**) production peaked at 4 – 5 days and 6 – 7 days, respectively. The observed drop of herbicidin A after 4–5 days was probably due to its susceptibility to hydrolysis as reported previously.¹⁹

The optimized purification protocol was then developed based on the procedures already reported in literature.^{18,19} EtOAc and *n*-BuOH can extract most of herbicidins A and B out of the filtered culture. The crude extracts can be further enriched with herbicidins by passing the extracts through Diaion HP-20 with gradient elution using aqueous MeOH (40 – 90%). A final silica-gel purification step with 5 – 2.5% MeOH in CH₂Cl₂ typically provided 5 – 10 mg yields of herbicidins A and B with good purity from a 100 mL culture. Figure S2 shows the ¹H NMR comparison of herbicidins isolated from the optimized protocol with those reported in the literature.¹⁸

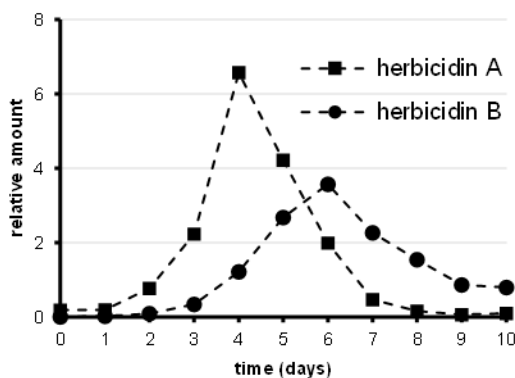


Figure S1. Production profiles of herbicidins A and B by *Streptomyces* sp. L-9-10 over 10 days.

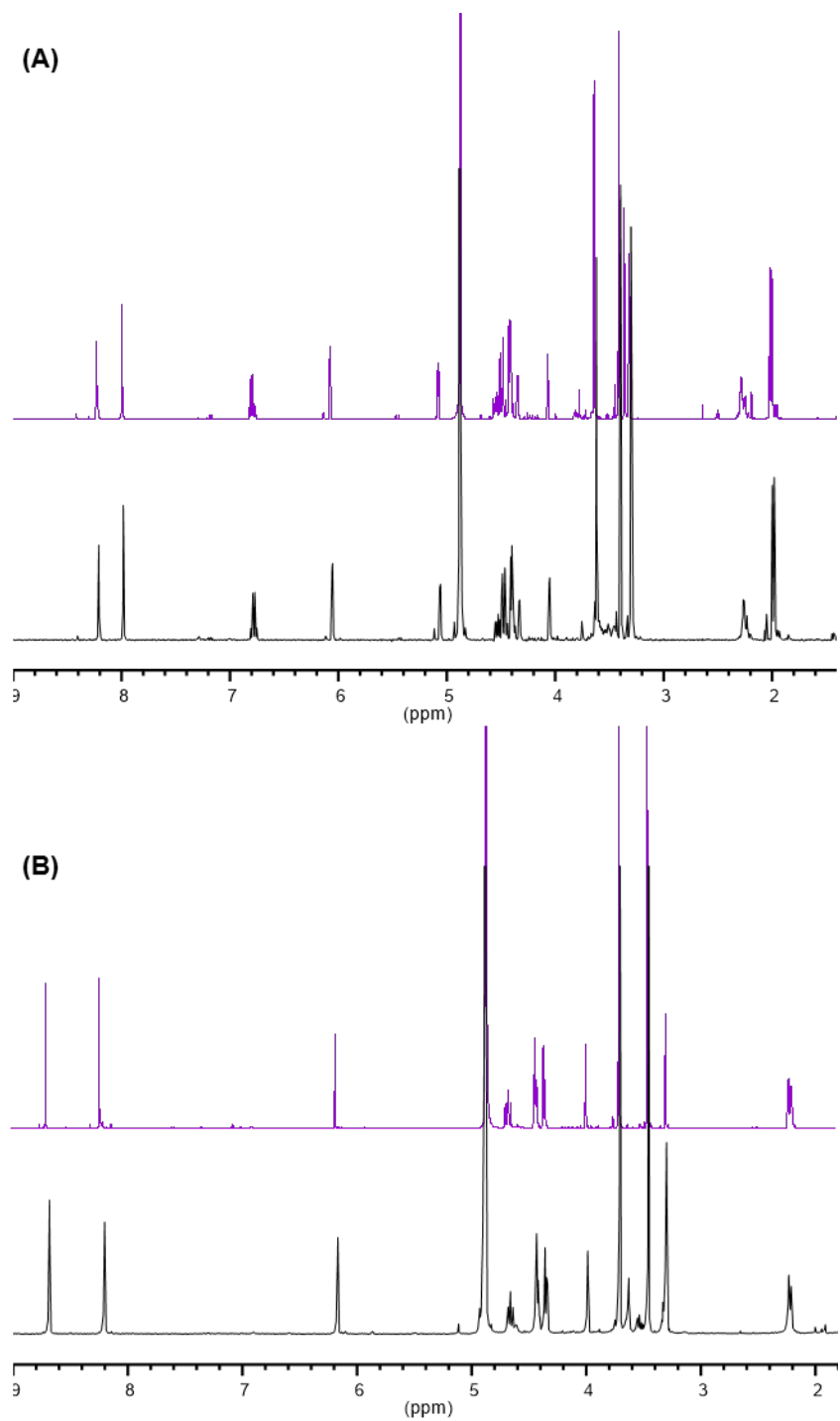


Figure S2. ^1H NMR of (A) herbicidin A and (B) herbicidin B in CD_3OD . The top spectrum in each subfigure is adapted from the literature,¹⁸ and the bottom spectrum is from herbicidins purified using the modified protocols described above.

S3. Feeding Studies

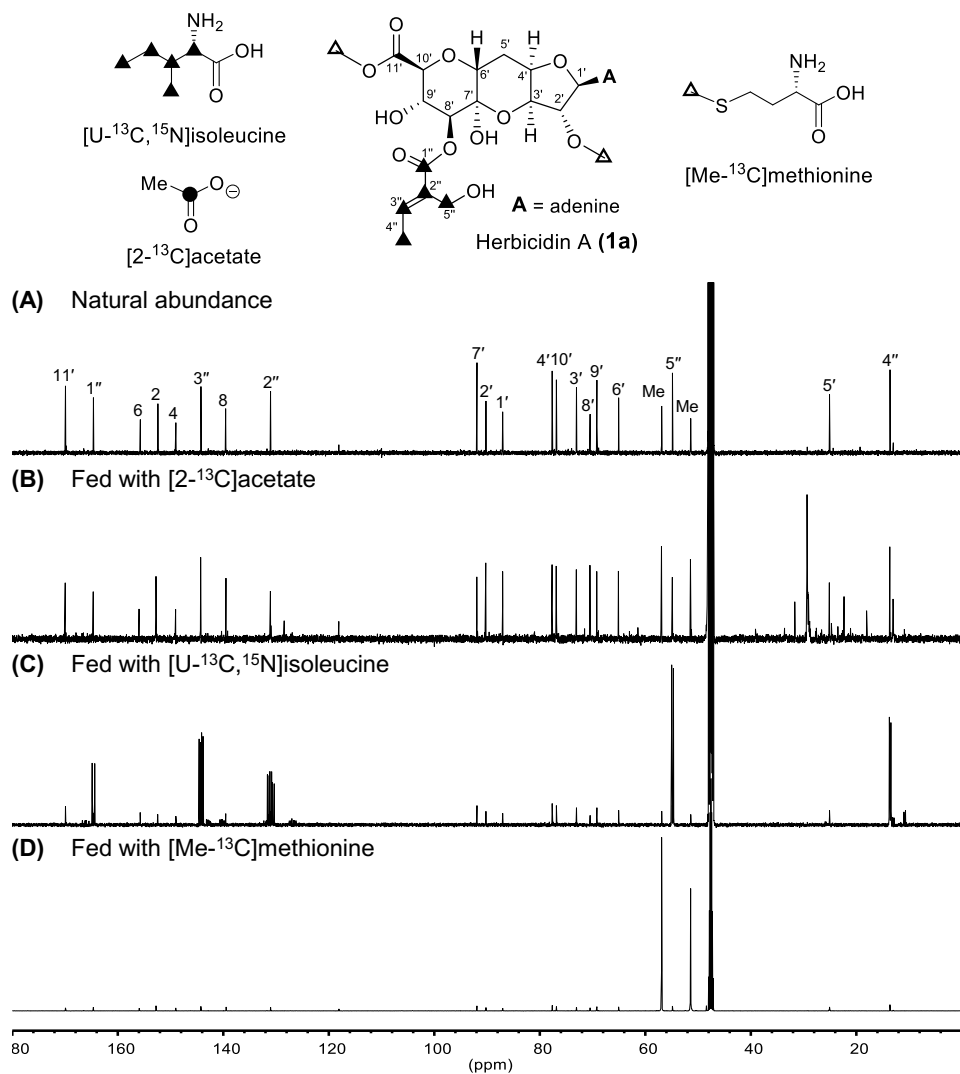
S3.1. Peripheral Modifications

Streptomyces sp. L-9-10 was fed with either [U-¹³C, ¹⁵N]isoleucine or sodium [2-¹³C]acetate in order to distinguish between the two possible pathways (catabolism of L-isoleucine versus polyketide machinery) during assembly of the tiglyl moiety in herbicidins. Analysis of ¹³C NMR spectra of herbicidin A isolated from the culture showed that all of the carbons on the hydroxy-tiglyl group were enriched with ¹³C indicating that they were derived from the labeled L-isoleucine (Figure S3C). Since these carbons are found in the same spin system, L-isoleucine must have been incorporated into herbicidin A as an intact entity without being fragmented (see table in Figure S3). On the other hand, although feeding *Streptomyces* sp. L-9-10 with [2-¹³C]acetate appeared to slightly perturb the ¹³C NMR spectrum of herbicidin A, no apparent ¹³C enrichment on the acyl side chain was observed (Figure S3B). This implies that biosynthesis of the tiglyl group in herbicidin A most likely utilizes the products of L-isoleucine catabolism instead of employing a polyketide-based machinery. In addition, enrichment of ¹³C at the two methyl groups of herbicidin A isolated from the culture fed with [Me-¹³C]methionine (Figure S3D) indicated the participation of two SAM-dependent methyltransferases in the biosynthesis of herbicidins.

S3.2. Core Assembly

When cultures were fed with [5-¹³C]ribose, ¹³C-enrichment of the C5' carbon of herbicidin A was noted (Figure S4B). Similarly, when cultures were fed with [U-¹³C]ribose, the C1' to C5' carbons were also found to be enriched as shown in Figure S4C. Analysis of the multiplicities of these ¹³C NMR signals is summarized in Figure S4D (solid lines) and the associated table. As in the case of L-isoleucine, the couplings patterns indicated membership within the same spin system suggesting that ribose or a derivative thereof is the immediate source of the A ring of herbicidin A and the C5' carbon of the B ring. Several minor coupling patterns with lower intensity were also discernible across the entire molecule as indicated by the dashed lines in Figure S4D. These additional couplings could potentially arise from the catabolism of [U-¹³C]ribose to [U-¹³C]acetate/pyruvate followed by gluconeogenesis to regenerate ¹³C-labeled glucose/ribose prior to incorporation into herbicidin A. Since this represents indirect incorporation, the couplings are not from the same spin system, and therefore, the enrichments would be less prominent.

A similar observation was also made when the culture was fed with labeled glucose, where the C6' and C11' carbons of herbicidin A were derived from C1 and C6 of D-glucose, respectively (Figure S5B and C). Furthermore, an intact spin system involving C6' to C11' was observed when [U-¹³C]glucose was supplied to the culture (Figure S5D and solid lines in Figure S5E), suggesting that the C ring of herbicidin A is derived from glucose. Analogous to the experiments with labeled ribose, several additional spin systems were observed in the herbicidin A isolated from cultures fed with ¹³C-labeled glucose as indicated by the dashed lines in Figure S5E. In Figure S5B, C1 of [1-¹³C]glucose is apparently also incorporated into C1' of herbicidin A. This additional enrichment may result from the interplay of primary metabolism (glycolysis, gluconeogenesis, pentose phosphate pathway, etc.) with the biosynthetic machinery of herbicidins.



Carbon	δ (ppm)	Multiplicity	J (Hz)
1''	164.6	br d	72.6
2''	131.0	ddd	72.6, 70.3, 49.5
3''	144.2	dd	70.3, 41.4
4''	13.6	ddd	41.4, 5.7, 3.5
5''	54.8	dt	49.5, 3.5

Figure S3. ¹³C NMR of herbicidin A isolated from cultures of *Streptomyces* sp. L-9-10 fed with labeled amino acids. The culture was fed with (A) no additive, (B) sodium [2-¹³C]acetate, (C) [U-¹³C, ¹⁵N]isoleucine, and (D) [Me-¹³C]methionine. The structures illustrate the ¹³C-enrichments observed in herbicidin A versus the labeled materials fed to the cultures. Assignments of ¹³C-enriched carbons in (C) are summarized in the table.

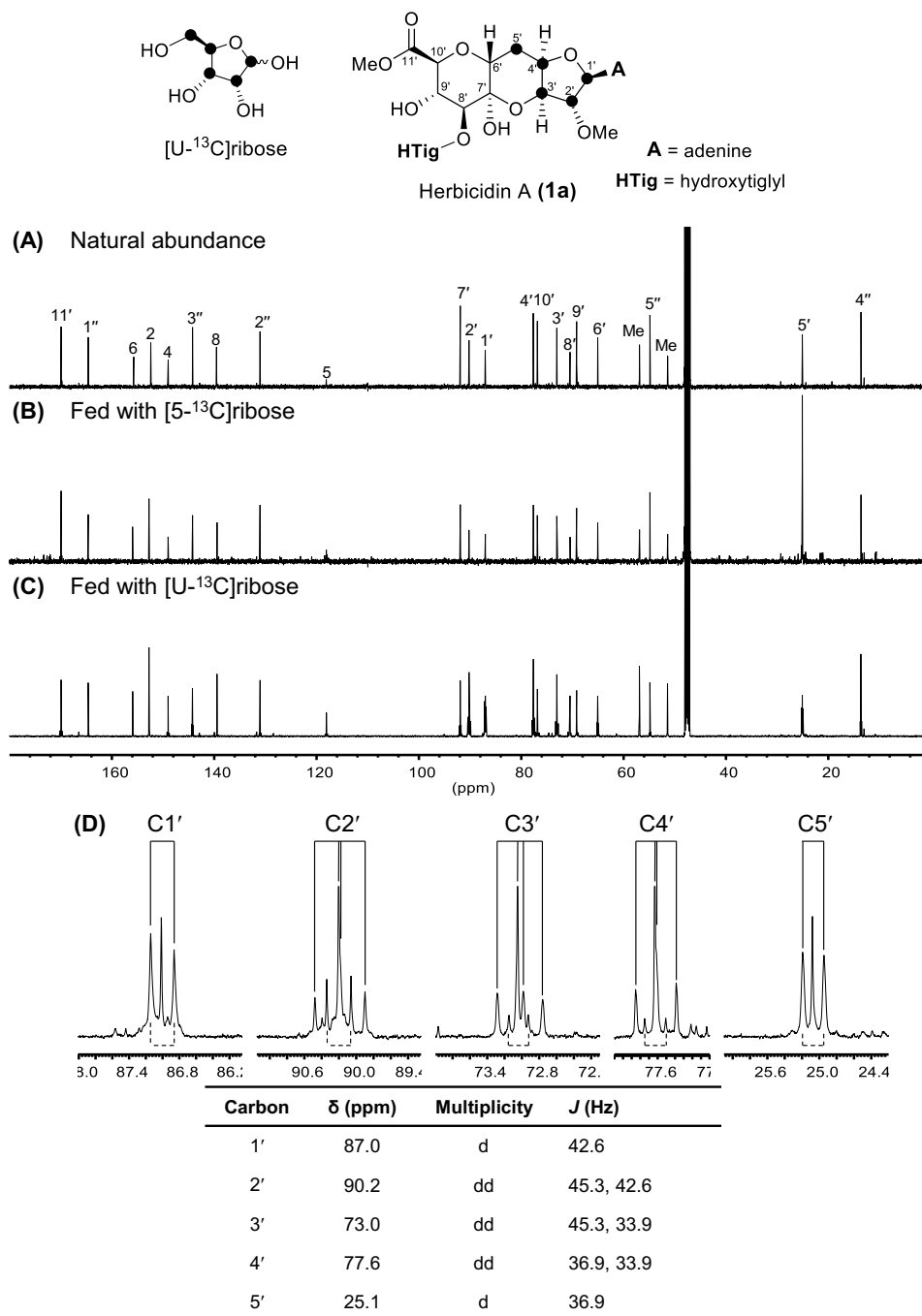


Figure S4. ¹³C NMR of herbicidin A isolated from a culture of *Streptomyces* sp. L-9-10 fed with labeled ribose. The culture was fed with **(A)** no additive, **(B)** [5-¹³C]ribose, or **(C)** [U-¹³C]ribose. The multiplicity analysis of C1' to C5' is shown in **(D)** and summarized in the associated table. The solid lines are the most prominent couplings resulting from the direct incorporation of labeled ribose. The dashed lines suggest indirect incorporation.

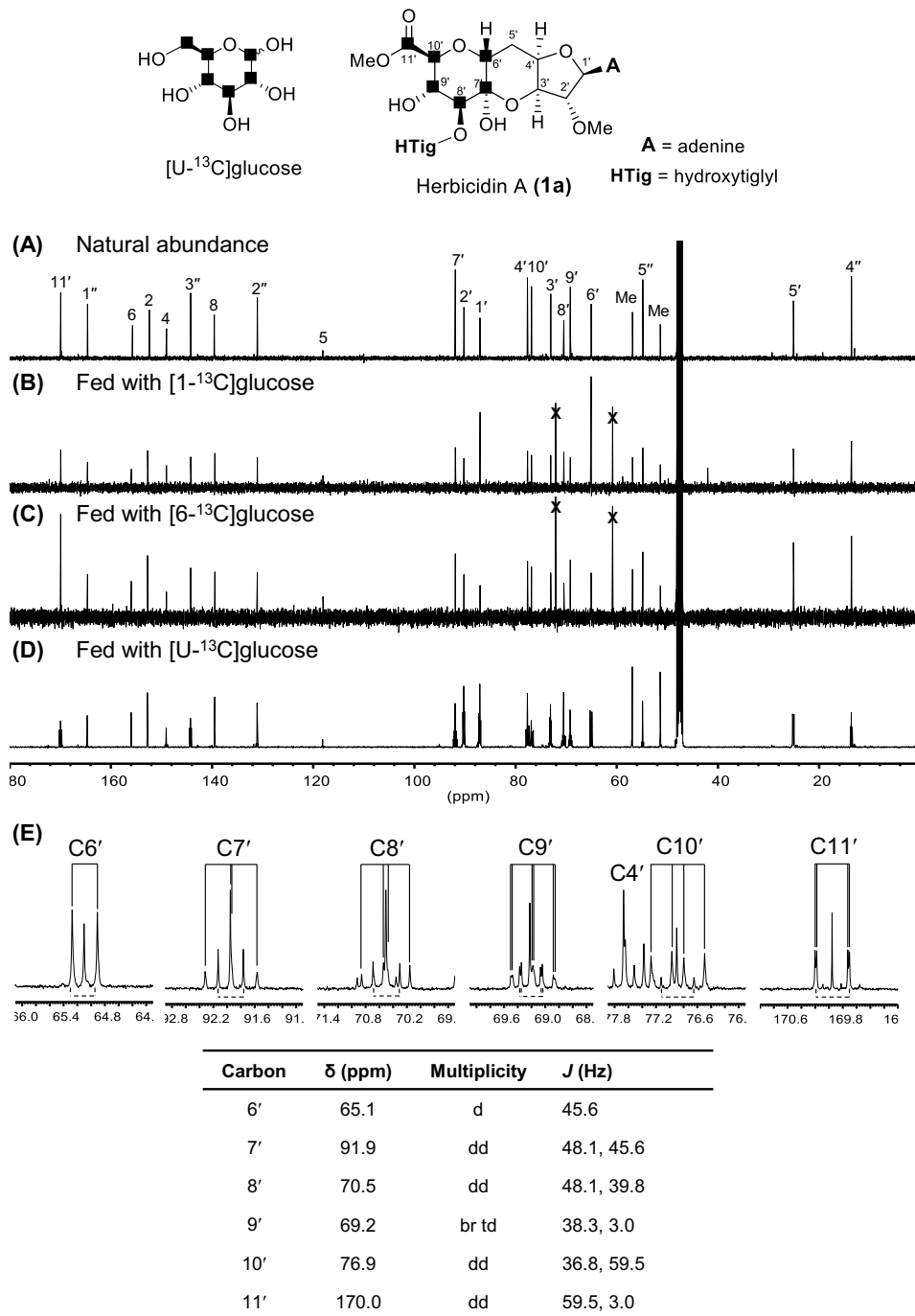


Figure S5. ¹³C NMR of herbicidin A isolated from a culture of *Streptomyces* sp. L-9-10 fed with labeled glucose. The culture was fed with (A) no additive, (B) [1-¹³C]glucose, (C) [6-¹³C]glucose, or (D) [U-¹³C]glucose. Multiplicity analysis of C6' to C11' is shown in (E) and summarized in the associated table. The solid lines are the most prominent couplings resulting from direct incorporation of labeled glucose. The dashed lines suggest indirect incorporation. The signals labeled with cross signs are from the contamination of glycerol.

S4. Identification of the Gene Cluster

The putative herbicidin biosynthetic cluster (*her*, Figure S6A) was identified by locating the two methyltransferases in close vicinity to each other as described in the main text. Annotations of these *her* genes by BLASTP and their predicted functions are summarized in Table S3. Through our BLAST analyses of the *her* gene cluster, we noticed that *Streptomyces scopuliridis* RB72 and *Streptomyces* NRRL F-5135 also had clusters of genes that showed high homology to *her3* – *her11* (generally 75 – 95% identical, Table S4) as shown in Figure S6B (*sco-her*) and Figure S6C (*5135-her*). *S. scopuliridis* RB72 is known to produce herbicidins as well,²⁰ further substantiating the identity of this cluster for the biosynthesis of herbicidins.

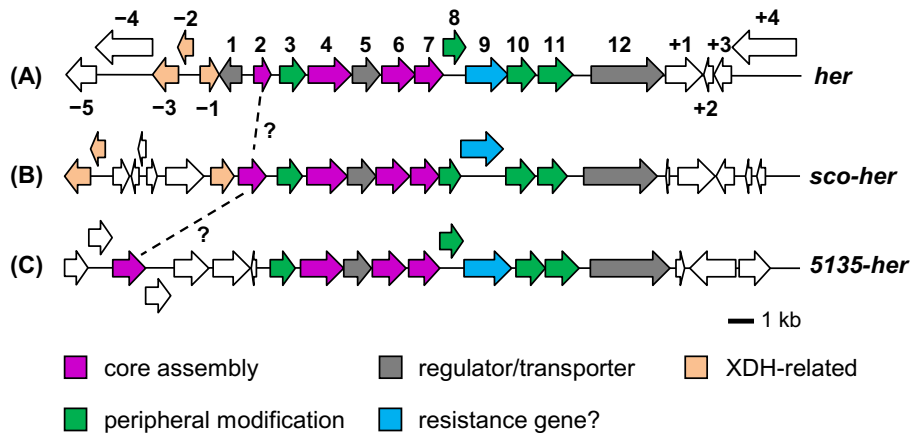


Figure S6. Putative biosynthetic gene clusters for the herbicidins from (A) *Streptomyces* sp. L-9-10, (B) *S. scopuliridis* RB72, and (C) *Streptomyces* NRRL F-5135.

Table S3. Annotation and predicted function of genes in the *her* cluster. *The length of predicted peptides. XDH: xanthine dehydrogenase. G3PDH: glyceraldehyde 3-phosphate dehydrogenase.

Gene	Size*	BLAST Annotation	Predicted Function
<i>orf-5</i>	383	XDH, maturation factor	
<i>orf-4</i>	733	XDH, Mo-binding subunit	
<i>orf-3</i>	331	XDH, FAD-binding subunit	
<i>orf-2</i>	200	XDH, [2Fe-2S]-binding subunit	
<i>orf-1</i>	241	TetR transcriptional regulator	
<i>her1</i>	284	XRE transcriptional regulator	transcriptional regulation?
<i>her2</i>	227	NAD-dependent epimerase	core – generation of 1i through 1k ?
<i>her3</i>	297	ketoacyl-ACP synthase III, FabH	peripheral – tiglyl attachment
<i>her4</i>	560	hypothetical / SAH hydrolase	core – C3' epimerization
<i>her5</i>	359	ABC transporter	transporter
<i>her6</i>	430	B12-dependent radical SAM enzyme	core – concatenation
<i>her7</i>	369	inositol 2-dehydrogenase	core – C7' oxidation
<i>her8</i>	287	SAM-dependent methyltransferase	peripheral – methylation
<i>her9</i>	543	serine hydrolase	resistance
<i>her10</i>	369	SAM-dependent methyltransferase	peripheral – methylation
<i>her11</i>	438	P450	peripheral – hydroxylation
<i>her12</i>	932	LuxR transcriptional regulator	transcriptional regulation
<i>orf+1</i>	482	G3PDH	
<i>orf+2</i>	120	hypothetical protein	
<i>orf+3</i>	227	histidine kinase	
<i>orf+4</i>	825	DNA-binding response regulator	

Table S4. Comparison of genes in the *her*, *sco-her*, and *5135-her* clusters. The numbers represent size / similarity / identity. *There is no *her2* homolog in *sco-her* and *5135-her*, so only the size of the closest dehydrogenase upstream of *her3* is shown.

Gene	size	<i>sco-her</i>	<i>5135-her</i>
<i>her2</i> *	227	430	361
<i>her3</i>	297	328 / 97% / 95%	328 / 91% / 86%
<i>her4</i>	560	520 / 97% / 95%	557 / 89% / 81%
<i>her5</i>	359	365 / 94% / 91%	360 / 80% / 75%
<i>her6</i>	430	435 / 97% / 96%	435 / 93% / 88%
<i>her7</i>	369	366 / 98% / 96%	401 / 91% / 84%
<i>her8</i>	287	281 / 92% / 90%	303 / 79% / 74%
<i>her9</i>	543	544 / 95% / 92%	606 / 81% / 76%
<i>her10</i>	369	374 / 95% / 93%	375 / 91% / 86%
<i>her11</i>	438	375 / 94% / 91%	440 / 82% / 76%
<i>her12</i>	932	940 / 88% / 83%	1026 / 63% / 52%

S5. Heterologous Expression

A pOJ446³-based cosmid library of *Streptomyces* sp. L-9-10 was constructed, and two sets of PCR primers were used to search for a cosmid that encodes the whole *her* gene cluster. Only one cosmid, L8B17, out of ca. 1,300 cosmids screened was identified as such as shown in Figure S7B and C. The boundary of L8B17 was determined by sequencing and mapped onto the draft genome. The cosmid encompasses segments of two contigs in the draft genome with a gap in between as depicted in Figure S7A.

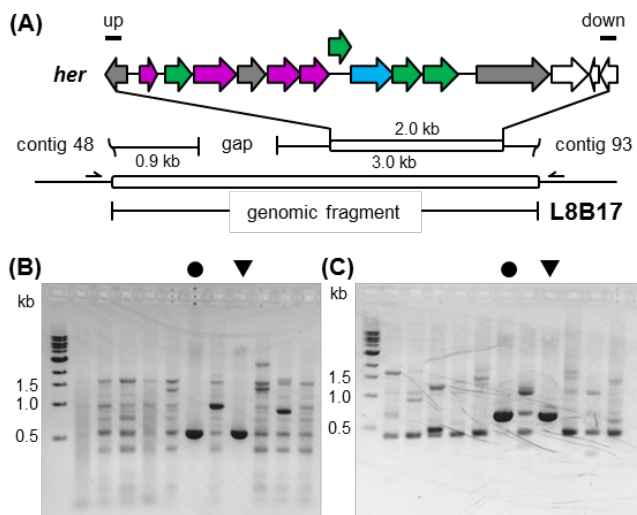


Figure S7. Identification of cosmid L8B17. (A) Schematic representation of cosmid L8B17 and agarose gel of screening cosmids using (B) up and (C) down probes. The *her* cluster is located near the 3'-end of the genomic fragment in L8B17. Two black bars on top of the gene cluster are the regions amplified by the PCR probes: up (GML01/02, 522 bp) and down (GML03/04, 630 bp). The two single-headed arrows are the primers (GML05/06, not scaled to the real sizes) used to determine the boundary of the genomic fragment. The first lane of each gel is the DNA ladder. The lanes labeled with ● and ▼ were generated using genomic DNA and cosmid L8B17 as the template in PCR reactions, respectively.

As described in the main text, heterologous host *Streptomyces albus* J1074 carrying cosmid L8B17 (Sa-L8B17) produced herbicides, while the same host carrying empty vector pOJ446 (Sa-pOJ446) did not. The HPLC traces of worked-up 10 day cultures of both strains are shown in Figure S8 along with the electrospray ionization-mass spectrometry (ESI-MS) confirmation of the two herbicides produced by Sa-L8B17.

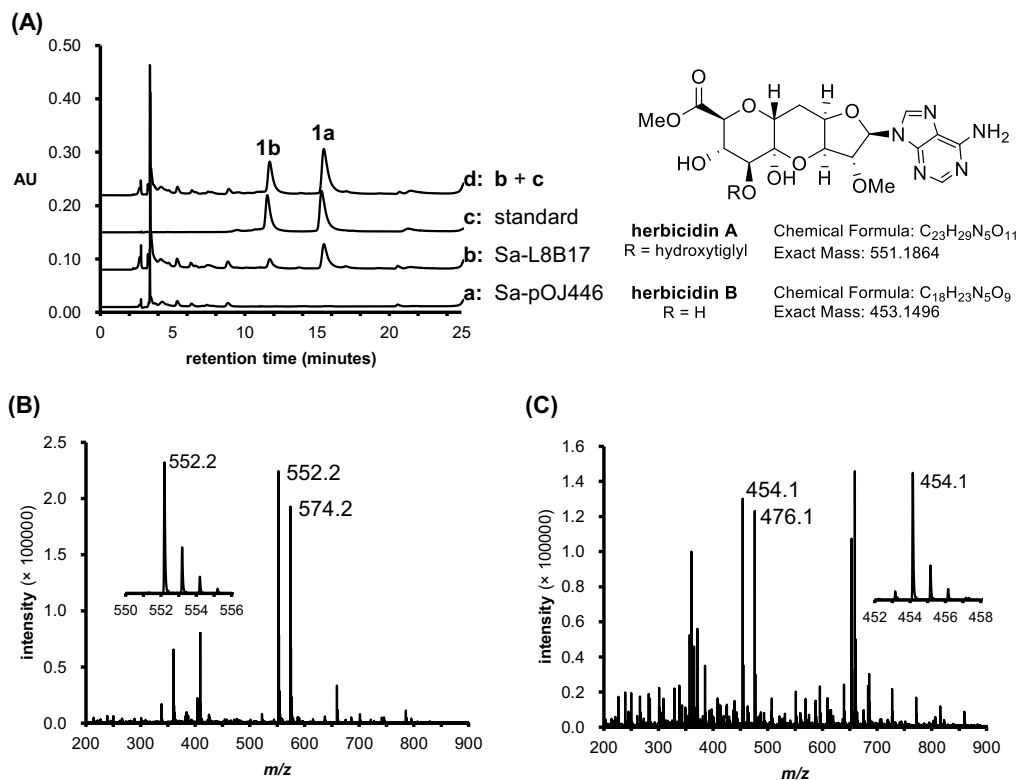


Figure S8. Heterologous expression of the *her* cluster in *S. albus* J1074. **(A)** HPLC traces of **a** 10 day extract of Sa-pOJ446, **b** 10 day extract of Sa-L8B17, **c** herbicidin standard, and **d** co-injection of the samples in traces **b** and **c**. **(B)** ESI-MS in positive ion mode of herbicidin A isolated from a 10 day extract of Sa-L8B17 culture by HPLC showing the protonated and sodiated adduct ions at 552.2 and 574.2, respectively. **(C)** ESI-MS in positive-ion mode of herbicidin B isolated from a 10 day extract of Sa-L8B17 culture by HPLC, showing the protonated and sodiated adduct ions at 454.1 and 476.1, respectively.

S6. Proposed Functions of Enzymes Encoded in the Cluster

The proposed biosynthetic pathway of herbicidins is shown in Figure 5. However, some of the enzymes are worthy of further discussion.

First, we expected an enzyme encoded in the cluster is involved in the condensation of herbicidin core with tiglyl-CoA; however, no apparent acyltransferase gene could be found in the cluster. On the other hand, *her3* encodes a ketoacyl-ACP synthase III (KASIII) that does not immediately seem pertinent to the biosynthesis of herbicidins.

KASIII typically catalyzes the Claisen-type condensation of malonyl-ACP and acetyl-CoA in fatty acid (FabH) and polyketide biosynthetic pathways.²¹ However, a few examples of KASIII that catalyze acyl-transfer reactions have been recently reported as shown in Figure S9. These enzymes can be categorized into two groups. In the first group, the acyl-donor is loaded onto a carrier protein before being transferred to the acceptor as observed in the biosyntheses of chlorothricin (**S3**)²² and clorobiocin (**S6**).²³ In contrast, enzymes of the second group catalyze activation of the acyl moiety as a CoA ester followed by direct condensation with an acceptor to form the ester linkage in cervimycin (**S9**)²⁴ and SF2575 (**S13**).²⁵ Given these reports, it is likely that Her3 acts like a KASIII-acyltransferase in the second group to catalyze attachment of the tiglyl moiety to the core of the herbicidins.

It should be noted, however, that Her3 actually shows higher homology to SsfN (58% identity, 74% similarity) versus SsfG (15% identity, 27% similarity). All these enzymes were annotated as KASIII by BLASTP, but SsfN was proposed to catalyze assembly of the angelyl-CoA ester (see Figure S9) rather than its condensation with an acceptor. Further investigation is needed to resolve this discrepancy.

Radical SAM enzymes comprise one of the largest enzyme superfamilies and feature the utilization of a 5'-deoxyadenosyl radical to catalyze a variety of transformations, including glyceryl radical generation, sulfur insertion, complex rearrangements, methylation, methylthiolation, dehydrogenation, C-X bond formation, C-X bond cleavage, metal cluster biosynthesis, etc.²⁶ Only a handful of B₁₂-dependent radical SAM have been characterized, with equally diverse activities. Therefore, it is proposed that Her6 is the key enzyme that couples the two sugar units together through a reaction mediated by radical chemistry (**3** + **4** → **6** in Figure 5).

After concatenation, we proposed that an epimerase is required to epimerize C3' of **6**. The assignment of Her2 as a C3' epimerase is tempting, but inconsistent with the apparent absence of a Her2 homolog in the *sco-her* and *5135-her* clusters (Table S4). Two nicotinamide adenine dinucleotide (NAD)-dependent enzymes are encoded upstream of *her3*: a tartrate dehydrogenase in *sco-her* and an inositol 2-dehydrogenase in *5135-her* (linked by dashed lines in Figure S6), which could possibly act as epimerases; however, they shared only a loose homology to each other.

The *her4* gene encodes a hypothetical protein that shows distant homology to S-adenosyl-L-homocysteine (SAH, **S14**) hydrolase. The C-terminus of Her4 features an NAD binding domain, but its N-terminus did not resemble the catalytic domain of SAH hydrolase.²⁷ The catalytic mechanism of SAH hydrolase is summarized in Scheme S1 and involves the reversible oxidation/reduction of the C3' hydroxyl of SAH and adenosine (**S14** ↔ **S15** and **S17** ↔ **S18**) by NAD to make the proton at C4' more acidic thereby facilitating an E1cB-type elimination of L-homocysteine from **S15** and subsequent hydration of the resulting methylene **S16**. Given the loose similarity between Her4 and SAH hydrolase as well as the presence of a NAD binding domain in Her4, it was hypothesized that the enzyme still retains the ability to oxidize the C3'-OH of **6**, but the hydride could come from either face to reduce C3'-O resulting in C3'-epimerization of **6**.

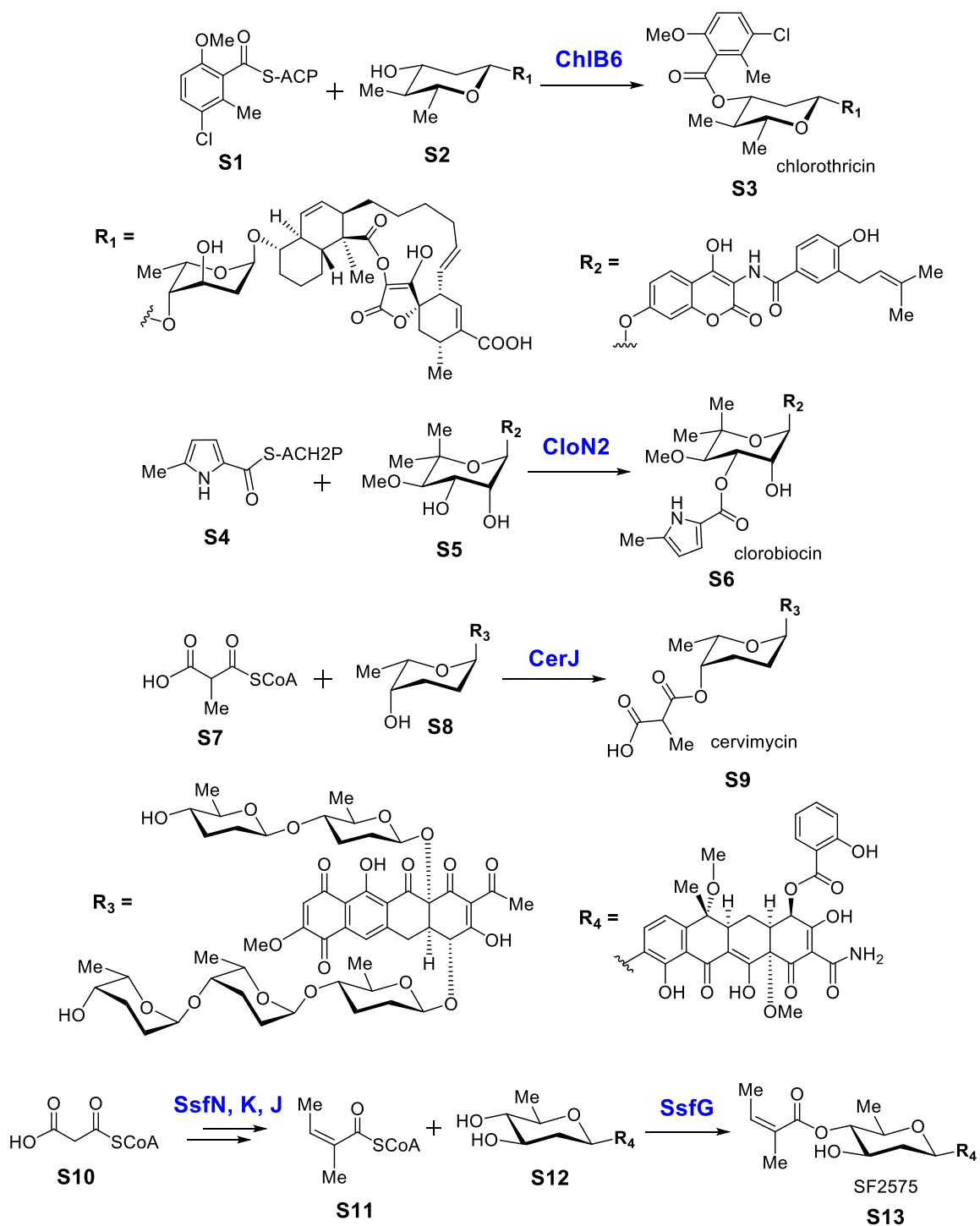
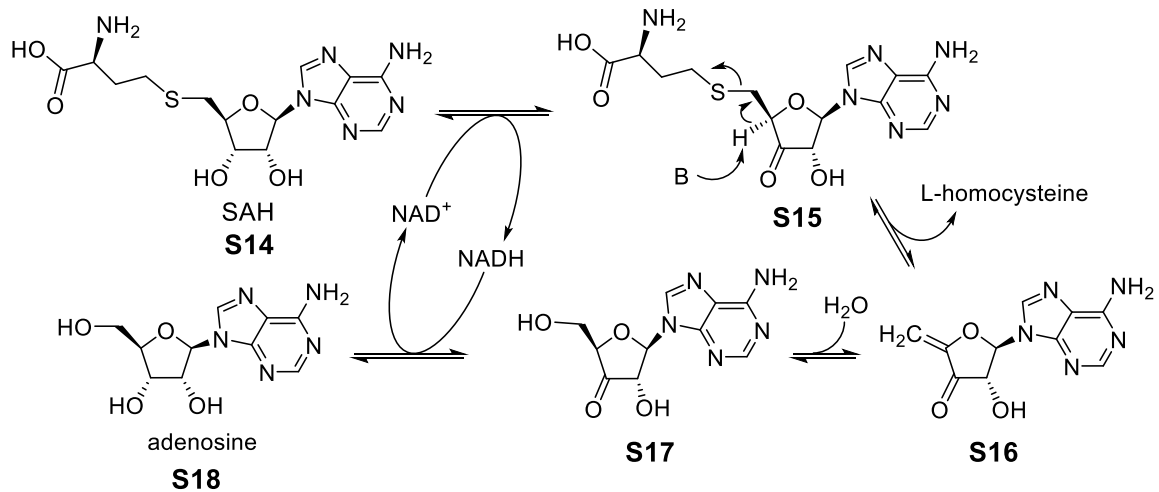


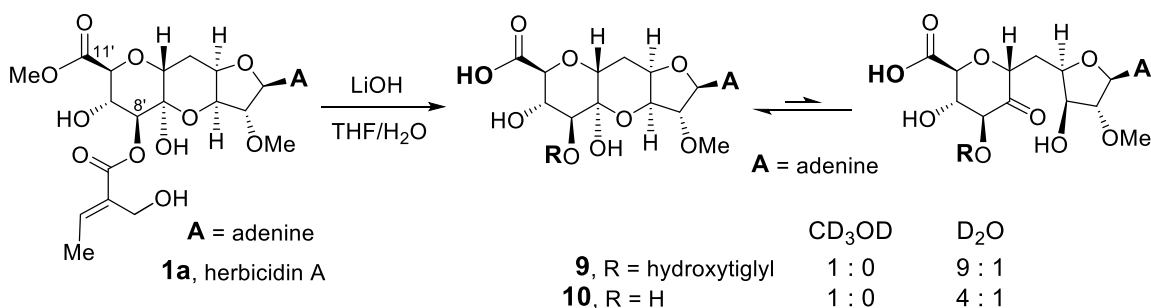
Figure S9. Enzymes annotated as KASIII catalyze acyl-transfer reactions.



Scheme S1. Catalytic mechanism of SAH hydrolase.

S7. Activity Assay of Methyltransferases

S7.1. Hydrolysis of Herbicidin A



Scheme S2. Hydrolysis of herbicidin A

Herbicidin A was hydrolyzed by LiOH in order to prepare putative substrates for the methyltransferase assays. By tuning the concentration of the reagent and the reaction time, it was possible to isolate two different products by HPLC: **9** and **10**. Interestingly, both compounds had only one set of ¹H NMR signals in CD₃OD, but another small set of signals was noted when the solvent was switched to D₂O (ca. 1 : 9 for **9**, and 1 : 4 for **10**. See Section S1.7 for assignment and Appendix for NMR spectra). The substituents at C8' to C10' of herbicidins are known to be axial, so the associated protons all have very small coupling constants (around 1 – 3 Hz).¹⁸ However, inspection of these small signals in **10** revealed greater coupling constants (around 9 – 10 Hz). This suggested that **10** was in equilibrium with its free carbonyl form (i.e., without the hemiacetal linkage) as shown in Scheme S2. In this case, the structure is not as rigid, and the glucuronic unit could be more flexible with all of its substituents pseudo-equatorial. This observation is consistent with the proposed biosynthetic pathway in which the hemiacetal linkage is formed non-enzymatically (see Figure 5 in the main text).

S7.2. Purification of Two Methyltransferases

Her8 could be overexpressed as an *N*-His₆-tagged protein and purified to near homogeneity as shown in Figure S10A. The maltose-binding protein (MBP)-fused Her10 (MBP-Her10) could be purified as soluble protein using an affinity column. Cleavage of MBP protein by TEV protease and subsequent purification yielded Her10 with high purity as shown in Figure S10B.

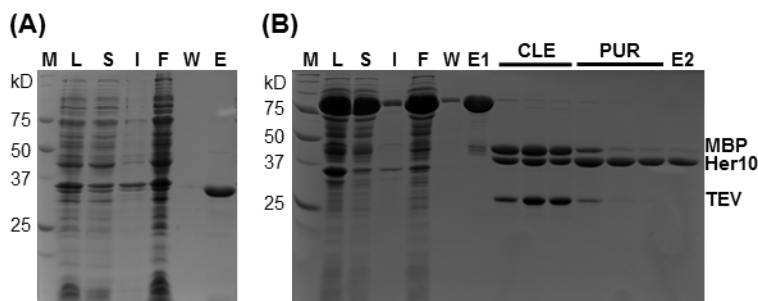


Figure S10. SDS-PAGE of the two purified methyltransferases. (A) *N*-His₆-tagged Her8 (33.1 kD, lane E), (B) MBP-Her10 (83.4 kD, lane E1), and Her10 (39.2 kD, lane E2). M: marker, L: whole-cell lysate, S: soluble fraction, I: inclusion bodies, F: flowthrough, W: washes, E: purified proteins, CLE: cleavage of MBP protein (samples taken from different time points), and PUR: removal of MBP and TEV by Ni-NTA column (samples taken from different rounds of purification).

S7.3. Activity Assay of Methyltransferases

The activity assays of two methyltransferases are described in the main text, and only the combination of **9** and Her8 showed the consumption of putative substrates. All of the HPLC traces including the co-injection of reaction mixture (Her8 + **9**) with standards and MS analysis of the reaction product are shown in Figure S11

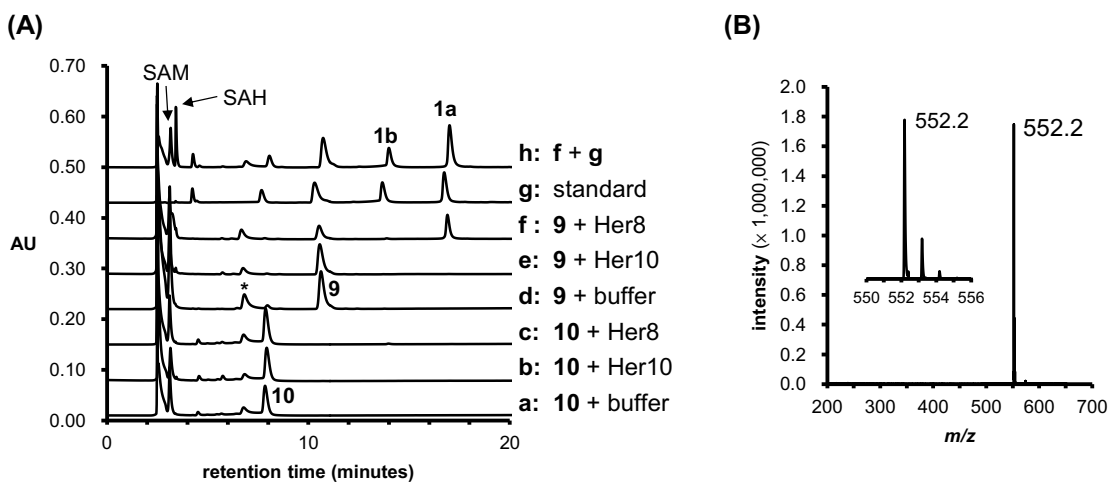
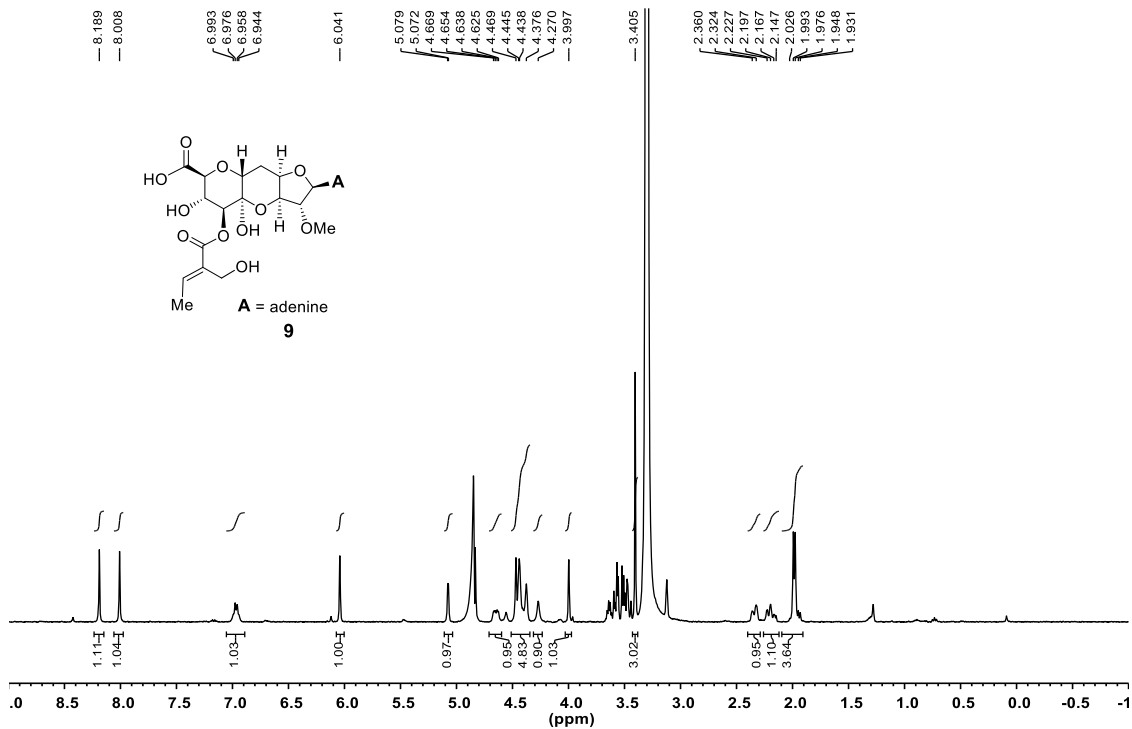
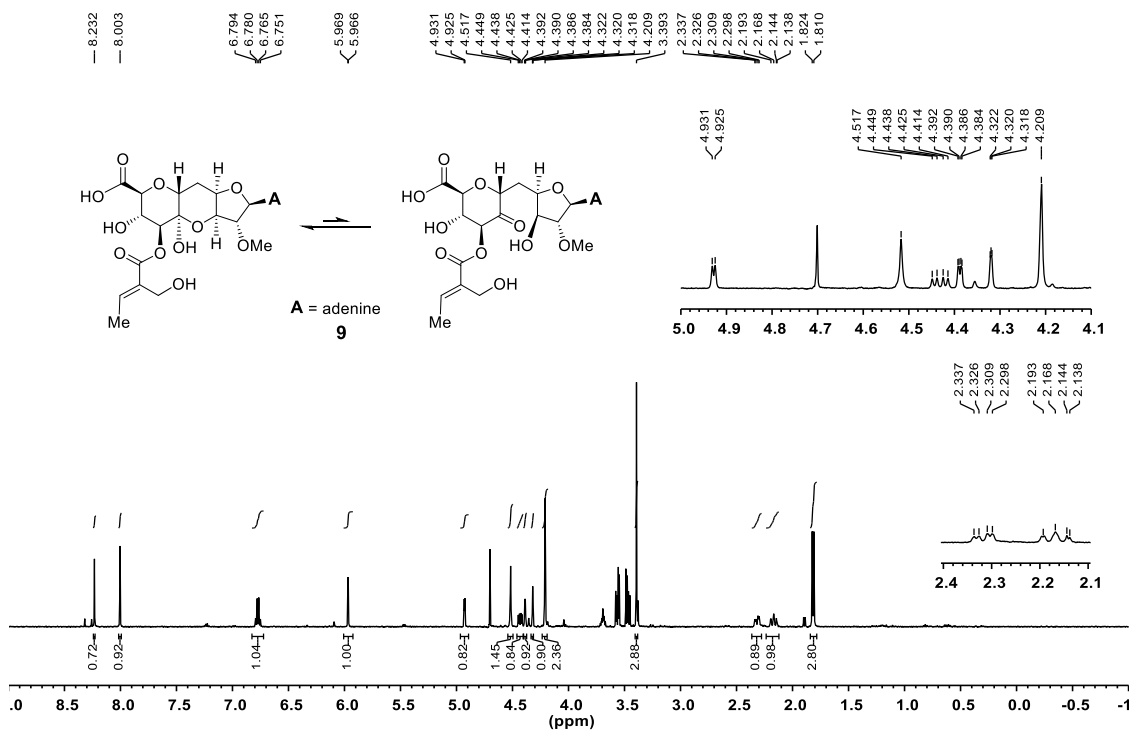
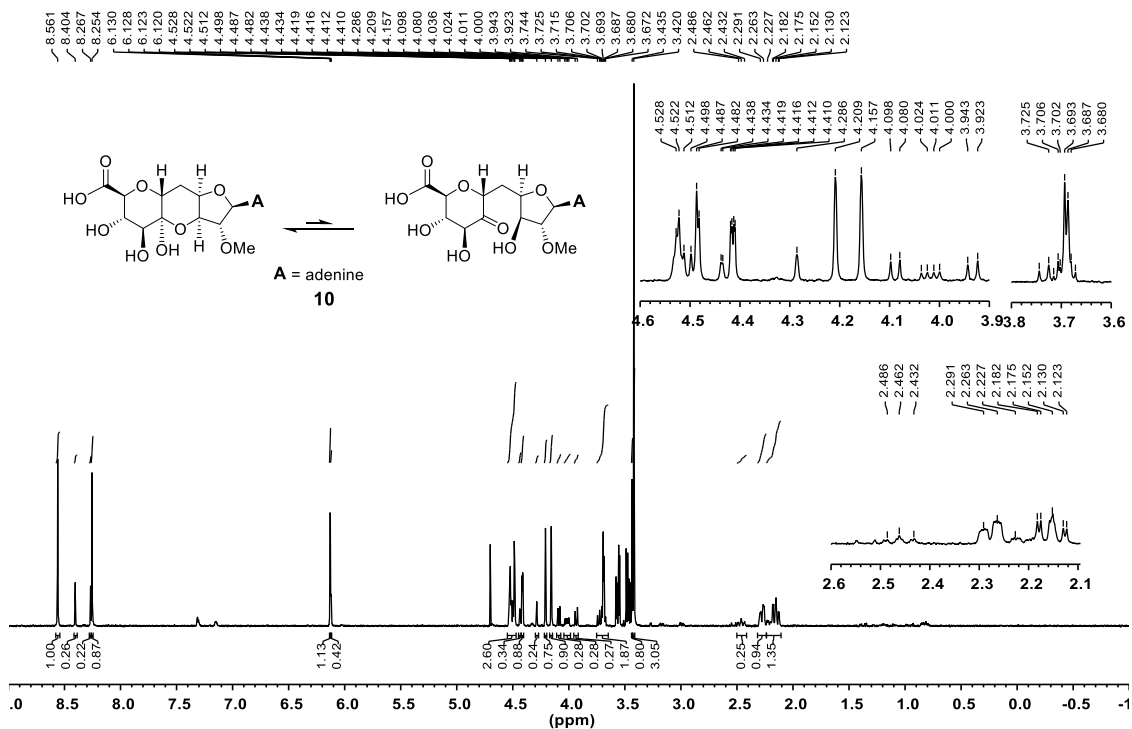


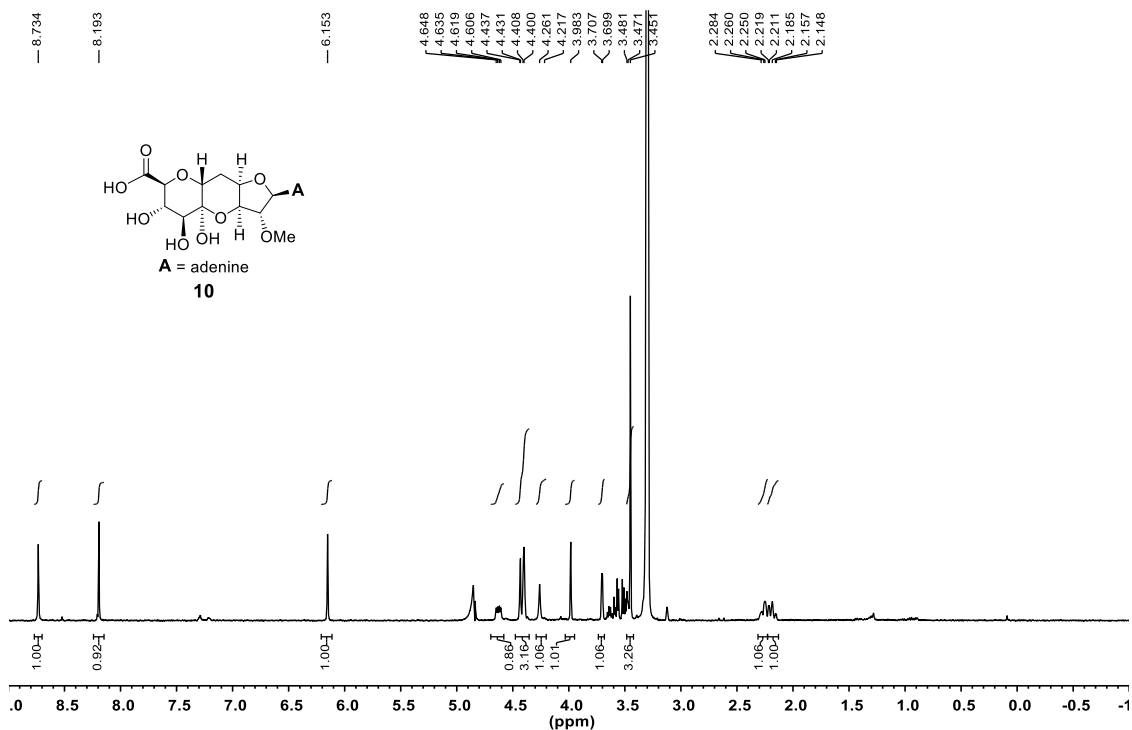
Figure S11. Activity assay of two methyltransferases, Her8 and Her10. **(A)** HPLC traces of the enzymatic assay. The combination of substrate and enzyme/buffer is indicated next to each trace. Trace **h** is a co-injection of the samples for traces **f** and **g** (herbicide standards). The peak labeled with asterisk is 5'-deoxy-5'-methylthioadenosine from the degradation of SAM. **(B)** ESI-MS in positive-ion mode of the product from the reaction of **9** and Her8. Predicted $[M + H]^+$ of herbicide A ($C_{23}H_{29}N_5O_{11}$, **1a**): 552.1936, found: 552.2.

Appendix (NMR Spectra)





¹H NMR (D₂O, 500 MHz) of 10



¹H NMR (CD₃OD, 500 MHz) of 10

S8. References

1. Kieser, T.; Bibb, M. J.; Buttner, M. J.; Chater, K. F.; Hopwood, D. A. *Practical Streptomyces Genetics*; The John Innes Foundation, 2000.
2. Simon, R.; Priefer, U.; Pühler, A. *Nat. Biotechnol.* **1983**, *1*, 784–791.
3. Bierman, M.; Logan, R.; O'Brien, K.; Seno, E.; Rao, R. N.; Schonher, B. *Gene* **1992**, *116*, 43–49.
4. Bushnell, B. BBMap short read aligner, and other bioinformatic tools. <https://sourceforge.net/projects/bbmap/>.
5. Zerbino, D. R.; Birney, E. *Genome Res.* **2008**, *18*, 821–829.
6. Gladman, S.; Seemann, T. 2012; <http://www.vicbioinformatics.com/software.velvetoptimiser.shtml>.
7. (a) Aziz, R. K.; Bartels, D.; Best, A. A.; Dejongh, M.; Dicz, T.; Edwards, R. A.; Formsma, K.; Gerdes, S.; Glass, E. M.; Kubal, M.; Meyer, F.; Olsen, G. J.; Olson, R.; Osterman, A. L.; Overbeek, R. A.; McNeil, L. K.; Paarmann, D.; Paczian, T.; Parrello, B.; Pusch, G. D.; Reich, C.; Stevens, R.; Vassieva, O.; Vonstein, V.; Wilke, A.; Zagnitko, O. *BMC Genomics* **2008**, *9*, 75. (b) Overbeek, R.; Olson, R.; Pusch, G. D.; Olsen, G. J.; Davis, J. J.; Disz, T.; Edwards, R. A.; Gerdes, S.; Parrello, B.; Shukla, M.; Vonstein, V.; Wattam, A. R.; Xia, F.; Stevens, R. *Nucleic Acids Res.* **2013**, *42*, D206–D214. (c) Brettin, T.; Davis, J. J.; Disz, T.; Edwards, R. A.; Gerdes, S.; Olsen, G. J.; Olson, R.; Overbeek, R.; Parrello, B.; Pusch, G. D.; Shukla, M.; Thomason, J. A. III; Stevens, R.; Vonstein, V.; Wattam, A. R.; Xia, F. *Sci. Rep.* **2015**, *5*, 8365.
8. (a) Medema, M. H.; Blin, K.; Cimermancic, P.; de Jager, V.; Zakrzewski, P.; Fischbach, M. A.; Weber, T.; Takano, E.; Breitling, R. *Nucleic Acids Res.* **2011**, *39*, W339–W346. (b) Blin, K.; Medema, M. H.; Kazempour, D.; Fischbach, M. A.; Breitling, R.; Takano, E.; Weber, T. *Nucleic Acids Res.* **2013**, *41*, W204–W212. (c) Weber, T.; Blin, K.; Duddela, S.; Krug, D.; Kim, H. U.; Brucoleri, R.; Lee, S. Y.; Fischbach, M. A.; Mller, R.; Wohlleben, W.; Breitling, R.; Takano, E.; Medema, M. H. *Nucleic Acids Res.* **2015**, *43*, W237–W243.
9. Simon, R.; Priefer, U.; Pühler, A. *Nat. Biotechnol.* **1983**, *1*, 784–791.
10. Baltz, R. H.; Matsushima, P. *J. Gen. Microbiol.* **1981**, *127*, 137–146.
11. Bradford, M. M. *Anal. Biochem.* **1976**, *72*, 248–254.
12. (a) Takatsuki, A.; Arima, K.; Tamura, G. *J. Antibiot. (Tokyo)* **1971**, *24*, 215–223. (b) Takatsuki, A.; Tamura, G. *J. Antibiot. (Tokyo)* **1971**, *24*, 224–231. (c) Takatsuki, A.; Kawamura, K.; Okina, M.; Kodama, Y.; Ito, T.; Tamura, G. *Agric. Biol. Chem.* **1977**, *41*, 2307–2309. (d) Ito, T.; Takatsuki, A.; Kawamura, K.; Sato, K.; Tamura, G. *Agric. Biol. Chem.* **1980**, *44*, 695–698.
13. (a) Uchida, K.; Ichikawa, T.; Shimauchi, Y.; Ishikura, T.; Ozaki, A. *J. Antibiot. (Tokyo)* **1971**, *24*, 259–262. (b) Uchida, K. *Agric. Biol. Chem.* **1976**, *40*, 395–404. (c) Ennifar, S.; Das, B. C.; Nash, S. M.; Nagarajan, R. *J. Chem. Soc., Chem. Commun.* **1977**, 41–42.
14. Tsvetanova, B. C.; Kiemle, D. J.; Price, N. P. *J. Biol. Chem.* **2002**, *277*, 35289–35296.
15. (a) Wyszynski, F. J.; Hesketh, A. R.; Bibb, M. J.; Davis, B. G. *Chem. Sci.* **2010**, *1*, 581–589. (b) Chen, W.; Qu, D.; Zhai, L.; Tao, M.; Wang, Y.; Lin, S.; Price, N. P. J.; Deng, Z. *Protein Cell* **2010**, *1*, 1093–1105.
16. Wyszynski, F. J.; Lee, S. S.; Yabe, T.; Wang, H.; Gomez-Escribano, J. P.; Bibb, M. J.; Lee, S. J.; Davies, G. J.; Davis, B. G. *Nat. Chem.* **2012**, *4*, 539–546.
17. Yoshikawa, H.; Takiguchi, Y.; Terao, M. *J. Antibiot. (Tokyo)* **1983**, *36*, 30–35.
18. Chai, X.; Youn, U. J.; Sun, D.; Dai, J.; Williams, P.; Kondratyuk, T. P.; Borris, R. P.; Davies, J.; Villanueva, I. G.; Pezzuto, J. M.; Chang, L. C. *J. Nat. Prod.* **2014**, *77*, 227–233.
19. Haneishi, T.; Terahara, A.; Kayamori, H.; Yabe, J.; Arai, M. *J. Antibiot. (Tokyo)* **1976**, *29*, 870–875.
20. (a) Choi, C. W.; Choi, J.-S.; Ko, Y. K.; Kim, C.-J.; Kim, Y. H.; Oh, J. S.; Ryu, S. Y.; Yon, G. H. *Bull. Korean Chem. Soc.* **2014**, *35*, 1215–1217. (b) Ha, S.; Lee, K. J.; Lee, S. I.; Gwak, H. J.; Lee, J.-H.; Kim, T.-W.; Choi, H.-J.; Jang, J.-Y.; Choi, J.-S.; Kim, C.-J.; Kim, J.-C.; Kim, H.

- H.; Park, H. W. *J. Microbiol. Biotechnol.* **2017**, *27*, 947–955.
21. Cronan, J. E.; Thomas, J. *Methods Enzymol.* **2009**, *459*, 395–433.
 22. Jia, X.-Y.; Tian, Z.-H.; Shao, L.; Qu, X.-D.; Zhao, Q.-F.; Tang, J.; Tang, G.-L.; Liu, W. *Chem. Biol.* **2006**, *13*, 575–585.
 23. Xu, H.; Kahlich, R.; Kammerer, B.; Heide, L.; Li, S.-M. *Microbiology* **2003**, *149*, 2183–2191.
 24. Bretschneider, T.; Zocher, G.; Unger, M.; Scherlach, K.; Stehle, T.; Hertweck, C. *Nat. Chem. Biol.* **2011**, *8*, 154–161.
 25. Pickens, L. B.; Kim, W.; Wang, P.; Zhou, H.; Watanabe, K.; Gomi, S.; Tang, Y. *J. Am. Chem. Soc.* **2009**, *131*, 17677–17689.
 26. Broderick, J. B.; Duffus, B. R.; Duschene, K. S.; Shepard, E. M. *Chem. Rev.* **2014**, *114*, 4229–4317.
 27. Yamada, T.; Takata, Y.; Komoto, J.; Gomi, T.; Ogawa, H.; Fujioka, M.; Takusagawa, F. *Int. J. Biochem. Cell Biol.* **2005**, *37*, 2417–2435.